J Appl Electrochem (2009) 39:1665–1670
DOI 10.1007/s10800-009-9856-8

ORIGINAL PAPER

# Synthesis of Ni nanoparticles by plasma-induced cathodic discharge electrolysis

**Manabu Tokushige · Tokujiro Nishikiori · Yasuhiko Ito**

Received: 29 May 2008 / Accepted: 24 February 2009 / Published online: 15 March 2009


**Abstract** Ni nanoparticles were synthesized by plasma-induced cathodic discharge electrolysis in LiCl–KCl–CsCl + $NiCl_2$ at 573 K under 1 atm of Ar atmosphere. Ni nanoparticles with diameters of around 100 nm were obtained from the melt. It was also confirmed that particles predominantly grow at the surface of the melt, especially the region just under the discharge. Taking into account the above results, a novel type plasma-induced electrolytic cell has been designed and constructed; it operated successfully, a rotating Ni metal disk anode being adopted in order for the formed particles to be quickly removed from the region just under the discharge and be continuously transferred to the inner wall of the cold container. By using this novel type plasma-induced electrolytic cell, Ni nanoparticles with diameters of around 50 nm could be obtained.

**Keywords** Plasma-induced molten salt electrolysis · Cathodic discharge electrolysis · Nanoparticles

M. Tokushige (✉)
Department of Applied Chemistry, Graduate School of Engineering, Doshisha University, Kyotanabe, Kyoto 610-0321, Japan
e-mail: eti1505@mail4.doshisha.ac.jp

T. Nishikiori
R&D Laboratory, I'MSEP Co., Ltd., Kyoto 610-0332, Japan

Y. Ito
Department of Environmental Systems Science, Faculty of Science and Engineering, Doshisha University, Kyotanabe, Kyoto 610-0321, Japan

## 1 Introduction

Metal nanoparticles with diameters smaller than 100 nm are of great interest because of their special electronic, catalytic, optical, and magnetic properties as compared with their bulk counterparts [1–3]. These special properties have been applied in various fields ranging from microelectronics to biochemical science [1–9]. For instance, magnetic nanoparticles such as Ni, Co, and Fe have attracted much attention because of both their unique fundamental properties and application in various fields [4–7]. As for Ni nanoparticles, they may be used as conductive inks [4], electrode materials in multilayer ceramic capacitors [5], magnetic storage media [6], and catalysts [7]. At present, metal nanoparticles are synthesized mainly through gas-phase and liquid-phase methods [1–9]. However, each method has its problems. For example, in the case of gas-phase methods such as PVD [3] and CVD [7, 8], the process of producing metal nanoparticles requires complex equipment. And in the case of liquid phase methods [1, 2], mass-production of metal nanoparticles is difficult.

Plasma-induced cathodic discharge electrolysis in molten salt medium has now been created and developed by the authors and their collaborators. The principle of plasma-induced cathodic discharge electrolysis is shown in Fig. 1. This method is a non-conventional electrolysis that utilizes the discharge generated between the cathode and a molten salt electrolyte. Even when the cathode is positioned just above the melt surface, plasma-induced stationary discharge makes continuous electrolysis possible under appropriate conditions, even under atmospheric pressure. The discharge is maintained by electron emission from the cathode, whereby atmospheric Ar gas is partially dissociated to form condensed plasma in the gas

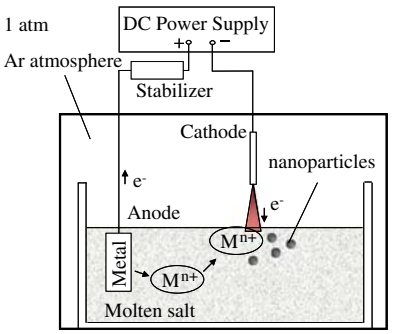


$M^{n+} + ne^- \rightarrow M$ (nanoparticle)

**Fig. 1** Principle of plasma-induced cathodic discharge electrolysis

phase. Therefore, when the metal ion source is dissolved in the melt, fine metal particles are formed in the melt whose sizes are in the nano- or micro-meter scale. In order to develop this method for industrial application, it is important to synthesize smaller and more uniform metal nanoparticles. From this aspect, the particle growth process was studied in detail [10–12]. At temperatures higher than 673 K, Kawamura et al. confirmed that the size of the particles obtained increased with rising bath temperature and quantity of electricity flowed, which suggests that particles collide and coalesce to form large particles, and that their sizes depend on the collision frequency between smaller particles [10, 11]. Oishi et al. suggested that the local temperature of the surface region of the melt just under the discharge is very high. In this region, the collision frequency was inferred to increase and particle growth was strongly promoted [12]. On the other hand, in previous studies [10–12], most of the particles were collected from the bottom part of the melt after a long period of electrolysis, though shortening of particle growth time, from a point in time of nucleation through a point in time of collection of grown particles, is considered necessary to obtain fine and uniform metal nanoparticles.

In this study, to obtain fine and uniform metal nanoparticles, the authors focus attention on continuous synthesis and quick collection of the metal nanoparticles. Firstly, in order to establish appropriate conditions for continuous synthesis and rapid collection of fine and uniform metal nanoparticles, we attempted to determine the region where particles predominantly grow. Taking into account the reports of Kawamura et al. that the sizes of the particles increased with rising bath temperature [10, 11], smaller and more uniform nanoparticles should be obtained at lower bath temperature. Then, in order to use a lower bath temperature than in the previous studies, LiCl–KCl–CsCl eutectic melt was used as solvent, and the formation of Ni particles in the melt containing Ni(II) ion (0.1 mol%) was conducted at 573 K.

## 2 Experimental procedure

The apparatus is shown in Fig. 2. A mixture of LiCl, KCl, and CsCl (LiCl:KCl:CsCl = 57.5:13.3:29.2 mol%; 99.9%, 99.5%, and 99.0% purity, respectively, Wako Pure Chemical Co., Ltd.) was dried at 473 K under vacuum for over 12 h and after melting at 573 K, pure Ar gas (99.998% purity, dew point: 208 K, Japan Air Gases Co., Ltd.) bubbling was conducted for 12 h. $NiCl_2$ (97.9% purity, Wako Pure Chemical Co., Ltd.) was used as the Ni(II) ion source. The cathode was a W rod (99.95% purity, Nilaco Co., Ltd.). The anode was a Ni plate (99.97% purity, Nilaco Co., Ltd.). The tip of the cathode was positioned at a few mm above the surface melt and the horizontal anode-cathode distance was around 15 mm (Fig. 2). The beaker was made of Pyrex glass. For stabilizing the discharge, a resistor was placed between the anode and a positive terminal of a DC power supply. Discharge was maintained by applying a few tens of volts

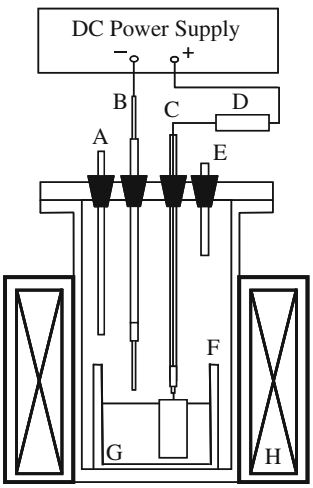


**Fig. 2** Scheme of experimental apparatus for plasma-induced cathodic discharge electrolysis. A Ar gas inlet, B Cathode, C Anode, D Stabilizer (resistor: 125 Ω), E Gas outlet, F Pyrex glass beaker, G LiCl–KCl–CsCl + $NiCl_2$ (0.1 mol%) melt, H Heater

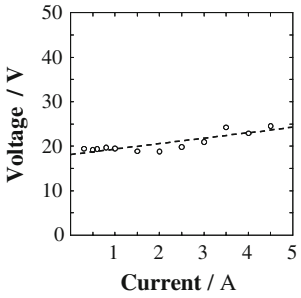


**Fig. 3** Voltages between the anode and the cathode at various currents

between the anode and the cathode. The voltages between the anode and the cathode at various currents are shown in Fig. 3. A linear relation between the voltage and the current was observed and the intercept of the fitted line was 18.1 V. In this study, the electrolysis was conducted at 1 A or 2 A. After electrolysis, the particles formed were collected and immersed in distilled water to remove the solidified salt. After drying, the particles were characterized by X-ray diffraction (XRD; Rigaku Co., RINT-2500), field emission scanning electron microscopy (FE-SEM; Hitachi Co., S-4300) and dynamic light scattering (DLS; Otsuka Electronics Co., MCLS-2000).

## 3 Results and discussions

### 3.1 Formation at 573 K

Figure 4 shows a typical XRD pattern of the product collected from the bottom after plasma-induced cathodic discharge electrolysis of 360 C at 1 A. The XRD pattern shows that the product only consists of Ni. An SEM image and the particle size distribution of the product are shown in Fig. 5a and b, respectively. Here, the particle size distribution based on the number is introduced, which shows the relative frequencies based on the number of each size class. The relative frequencies are defined by Eq. 1:

$$q_i = \frac{n_i}{\sum n_i} \quad (1)$$

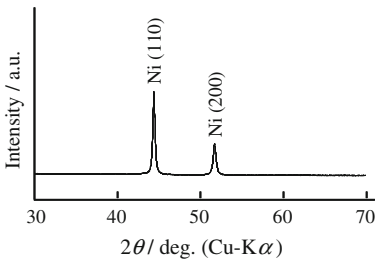


**Fig. 4** X-ray diffraction pattern of the product obtained by plasma-induced cathodic discharge electrolysis with 1 A for 6 min in LiCl–KCl–CsCl + $NiCl_2$ (0.1 mol%) at 573 K. Quantity of electricity: 360 C

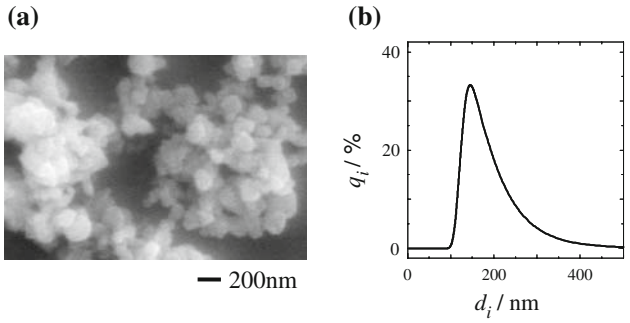


**Fig. 5** SEM image (**a**) and number base particle size distribution (**b**) of the product obtained by plasma-induced cathodic discharge electrolysis with 1 A for 6 min in LiCl–KCl–CsCl + $NiCl_2$ (0.1 mol%) at 573 K. Quantity of electricity: 360 C

where $q_i$ and $n_i$ denote the relative frequency and the number of particles classified into class i, respectively. The vertical axis of particle size distribution is relative frequency, $q_i$ defined by Eq. 1. The horizontal axis is the particle size, $d_i$. In the SEM image, nanoparticles with diameters of around 100 nm were observed. In the particle size distribution, it was also observed that the sizes of most particles were around 130 nm. So it was confirmed that Ni nanoparticles with diameters much smaller than those obtained at higher temperature than 673 K were formed [10]. The yield of Ni nanoparticles $\eta$ calculated from the total quantity of collected particles and Faraday's law was 79.5% for the passage of 360 C.

### 3.2 Region of particle growth

#### *3.2.1 Growth process*

Although the growth process of initially deposited metal atom clusters towards nanoparticles has not yet been completely clarified, this might be explained by collision and coalescence. Then, it is to be supposed that initially deposited metal atom clusters descend from the surface region of the melt to the bottom part while growing to form fine particles. In order to determine the critical region where the fine particles predominantly grow, the authors classified the melt into three regions as shown in Fig. 6, and collected particles from each region. Here, Region A is the surface region of the melt just under the discharge. The temperature of Region A is locally high, hence the collision frequency there is high and the particles may predominantly grow. Region B is the middle part of the melt. In this region, the particles descend from the surface region to the bottom part of the melt as they collide with each other. Region C is the bottom part of the melt. In this region, accumulated particles stay and maintain contact with each other for a long period.

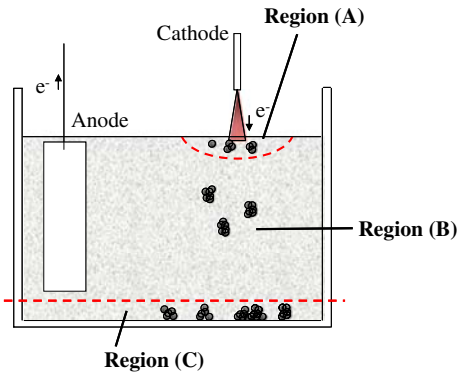


**Fig. 6** Classification of the region of particle growth. Region A: surface region of the melt just under the discharge, Region B: middle part of the melt, Region C: bottom part of the melt

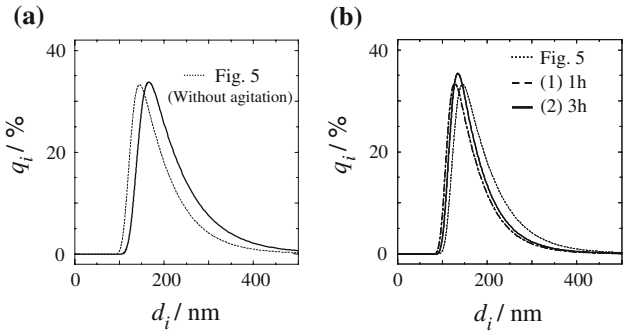


**Fig. 8** Number base particle size distributions of Ni nanoparticles obtained by plasma-induced cathodic discharge electrolysis with 1 A for 6 min in LiCl–KCl–CsCl + $NiCl_2$ (0.1 mol %) at 573 K. Quantity of electricity: 360 C. Collection time: **a** immediately **b** 1 h and 3 h after the electrolysis

### 3.2.2 *Bottom part of melt (Region C in Fig. 6)*

If the particles grow in Region C by contact with each other, the particle size should increase with length of the residence time there. In order to investigate the relation between the particle size and the residence time in Region C, particles were collected from the bottom while the electrolysis time was varied.

SEM image and particle size distribution of Ni nanoparticles (1 A, 3,600 C) are shown in Fig. 7a and b, respectively. The electrolysis time was tenfold longer than that of Fig. 5, which means the residence time in Region C was also longer. In Fig. 7, though the residence time in Region C was longer, both the particle sizes and the particle size distribution of Ni nanoparticles completely correspond to those of Fig. 5. These results indicate that the particle growth progresses little in Region C.

### 3.2.3 *Middle part of the melt (Region B in Fig. 6)*

If the particles grow in Region B by collision, the particle size should increase with residence time. Here, the residence time is the time since the particles are descending. In order to investigate the particle growth in Region B, the relation between the particle size and the residence time was observed, whereby the accumulation of particles was reduced by the agitation of the melt with Ar gas bubbling of 100 mL $min^{-1}$. Some particles were partly collected immediately after electrolysis and the others were collected 1 h and 3 h after electrolysis. Agitation of the melt was continued after the electrolysis was finished.

The particle size distribution obtained immediately after electrolysis (1 A, 360 C) is shown in Fig. 8a. The particle size distribution with agitation is broader than that of Fig. 5. This is because the particle growth in Region A was also promoted by agitation during electrolysis. Then, particle size distributions obtained 1 and 3 h after electrolysis were measured; the results are shown in Fig. 8b. In spite of the longer residence time, little difference among them is observed. Also, the particle size distributions are narrower than those of Figs. 5 and 8a. From the result that the particle sizes are smaller than those of Fig. 8a by residence in the agitated melt and the particle sizes do not change further with subsequent longer residence time than 1 h, it is indicated that particle growth does not progress in Region B after electrolysis. Therefore, it is suggested that particle growth predominantly progresses in Region A, and progresses little in the other parts of the melt.

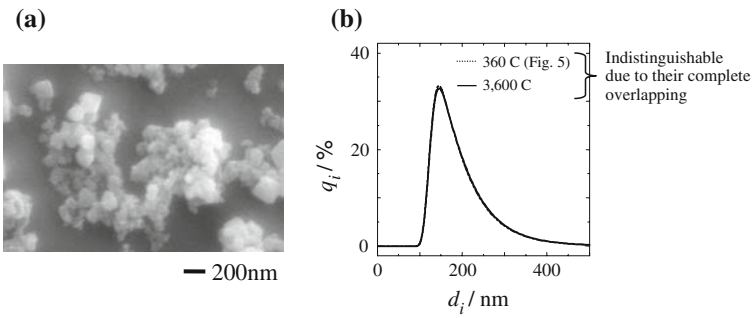


**Fig. 7** SEM image (**a**) and number base particle size distribution (**b**) of Ni nanoparticles obtained by plasma-induced cathodic discharge electrolysis with 1 A for 60 min in LiCl–KCl–CsCl + $NiCl_2$ (0.1 mol%) at 573 K. Quantity of electricity: 3,600 C

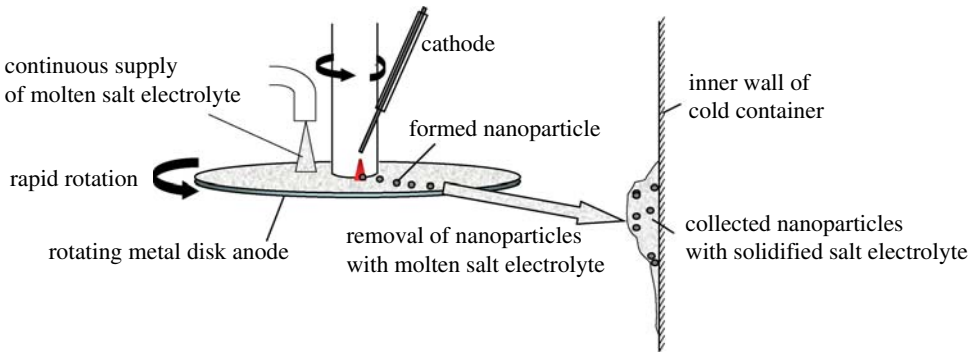


**Fig. 9** Schematic drawing of novel type plasma-induced electrolytic cell

### 3.3 Novel electrolytic cell for smaller and more uniform particles

The above results suggest that particles predominantly grow in Region A of the melt, the temperature of which is 573 K. Therefore, by rapid removal of the particles from Region A immediately after deposition, smaller and more uniform nanoparticles should be obtained. Taking into account the above results and considerations, a novel type plasma-induced electrolytic cell was designed and constructed. The scheme of this cell is shown in Fig. 9. The molten electrolyte is continuously supplied onto the surface of the rapidly rotating metal disk anode and is quickly removed from the vicinity of the cathode, thereby minimizing residence time in Region A by centrifugal force generated by the rotation of the disk. Here, for a few seconds, while the supplied electrolyte is removed from the disk to the inner wall of the cold container, by conducting plasma-induced cathodic discharge electrolysis in the electrolyte film with a thickness of a few mm, the initially deposited particles are quickly removed from the region just under the discharge (Region A in Fig. 6) and are continuously transferred to the inner wall of the cold container.

An SEM image and particle size distribution of Ni nanoparticles obtained using the novel electrolytic cell (rotation speed of anode disk: 500 rpm) are shown in Fig. 10a and b, respectively. In Fig. 10a, many Ni nanoparticles with diameters less than 50 nm were observed, and the particle size distribution is considerably narrower as seen in Fig. 10b. Thus smaller and more uniform Ni nanoparticles were successfully obtained using this novel electrolytic cell.

## 4 Conclusion

Ni nanoparticles were synthesized by plasma-induced cathodic discharge electrolysis in LiCl–KCl–CsCl + $NiCl_2$ at 573 K under 1 atm Ar atmosphere.

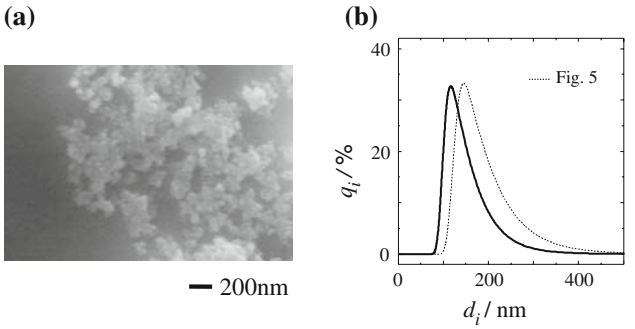


**Fig. 10** SEM image (**a**) and number base particle size distribution (**b**) of Ni nanoparticles obtained by using the novel plasma-induced electrolytic cell with 2 A in LiCl–KCl–CsCl + $NiCl_2$ (0.1 mol%)

Using a conventional type plasma-induced electrolytic cell, Ni nanoparticles with diameters of around 100 nm were obtained from the bottom part of the melt. Their sizes were smaller than those obtained in previous work conducted at temperatures higher than 673 K. It was also confirmed that particles predominantly grow in the surface region of the melt, especially the region just under the discharge, and grow little in the inner part of the melt at 573 K. Hence, synthesis of smaller and more uniform nanoparticles requires rapid removal of the particles from the region just under the discharge immediately after deposition.

Taking into account the above results and considerations, a novel type plasma-induced electrolytic cell was designed and constructed; a rotating Ni metal disk anode was adopted in order for the formed particles to be quickly removed from the region just under the discharge and be continuously transferred to the inner wall of the cold container. With the use of this novel plasma-induced electrolytic cell, Ni nanoparticles with diameters of less than 50 nm, with narrow particle size distribution, were obtained.

**Acknowledgment** This study was partly supported by a Grant-in-aid for scientific research from the Ministry of Education, Culture, Sports, Science and Technology (MEXT) of Japan, and by the Japan

Science and Technology Agency (JST) in Research for Promoting Technological Seeds.

## References

1. Puntes VF, Krishnan KM, Alivisatos AP (2001) Science 291:2115
2. Curtius J (2006) C R Physique 7:1027
3. Becker MF, Brock JR, Cai H, Henneke DE, Keto JW, Lee J, Nichols WT, Glicksman HD (1998) NanoStruct Mater 10:853
4. Tseng WJ, Chen CN (2006) J Mater Sci 41:1213
5. Chen W, Li L, Qi J, Wang Y, Gui Z (1998) J Am Ceram Soc 81:2751
6. Lok JGS, Geim AK, Maan JC, Dubonos SV, Kuhn LT, Lindelof PE (1998) Phys Rev B 58:12201
7. Yoshinaga M, Takahashi H, Yamamoto K, Muramatsu A, Morikawa T (2007) J Colloid Interface Sci 309:149
8. Qin C, Coulombe S (2007) Plasma Source Sci Technol 16:240
9. Magnusson MH, Deppert K, Malm JO (2000) J Mater Res 15:1564
10. Kawamura H, Moritani K, Ito Y (1998) J Jpn Soc Powder Powder Metall (Jpn) 45:1142
11. Kawamura H, Moritani K, Ito Y (1998) Plasmas Ions 1:29
12. Oishi H, Kawamura H, Ito Y (2002) J Appl Electrochem 32:819